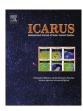


#### Contents lists available at ScienceDirect

## **Icarus**

journal homepage: www.elsevier.com/locate/icarus



# Electrostatic environment near lunar vertical hole: 3D plasma particle simulations



Yohei Miyake a,\*, Masaki N. Nishino b

- <sup>a</sup> Graduate School of System Informatics, Kobe University, Kobe, Japan
- <sup>b</sup> Solar-Terrestrial Environment Laboratory, Nagoya University, Nagoya, Japan

#### ARTICLE INFO

Article history: Received 16 March 2015 Revised 21 June 2015 Accepted 13 July 2015 Available online 18 July 2015

Keywords: Moon Moon, surface Solar wind

#### ABSTRACT

The dayside electrostatic environment near the lunar surface is governed by interactions among the solar wind plasma, photoelectrons, and the charged lunar surface, providing topologically complex boundaries to the plasma. Three-dimensional, particle-in-cell simulations are applied to recently discovered vertical holes on the Moon, which have spatial scales of tens of meters and greater depth-to-diameter ratios than typical impact craters. The vertical wall of the hole introduces a new boundary for both photo and solar wind electrons. The current balance condition established at a hole bottom is altered by the limited solar wind electron penetration into the hole due to loss at the wall and photoelectron current path connecting the hole bottom and wall surfaces. The self-consistent modeling not only reproduces intense differential charging between sunlit and shadowed surfaces, but also reveals the potential difference between sunlit surfaces inside and outside the hole, demonstrating the uniqueness of the near-hole electrostatic environment.

© 2015 Elsevier Inc. All rights reserved.

#### 1. Introduction

The Japanese lunar explorer Kaguya (SELENE) has recently revealed the existence of vertical holes on the Moon, which are possible lava tube skylights (Haruyama et al., 2009, 2012). The Kaguya and later observations by the Lunar Reconnaissance Orbiter (e.g., Robinson et al., 2012) have identified the diameters and depths of the holes as ranging from 50 to 100 m. Their depth-to-diameter ratios are much greater than those of typical impact craters (e.g., Pike, 1974). The holes can be interesting resources for geological study of the Moon, because their vertical walls, which are not covered by thick regolith layers unlike other lunar surfaces, should provide important clues for revealing the complex volcanic history of the Moon. The holes also have high potential as locations for constructing future lunar bases. Because of the high vertical walls, fewer extra-lunar rays/particles and micrometeorites can reach the hole bottoms than outside the holes. In this sense, these holes are not only of significance in selenology, but are also interesting from the viewpoint of electrostatic environments. The environments should be assessed before future landing missions are undertaken.

The electrostatic environment near the lunar surface is subject to plasma-surface interactions due to its exposure to both solar ultraviolet (SUV) radiation and solar wind electrons and protons. The surface charging is greatly influenced by the complex topography of the lunar surface, which can produce local shadowing of the SUV and solar wind plasma. Prior works have predicted mini-wake formation behind small obstacles (Farrell et al., 2007, 2010; Zimmerman et al., 2011) as well as supercharging near the interface between sunlit and shadowed regions (De and Criswell, 1977; Criswell and De, 1977; Wang et al., 2007; Farrell et al., 2010). Such a complex electrostatic environment creates a strong local electric field near the surface, which is considered to play an important role in the transport of charged dust grains on the Moon (Stubbs et al., 2007; Farrell et al., 2007; Wang et al., 2010).

The present work investigates the electrostatic plasma environment around a lunar vertical hole on the lunar dayside, using three-dimensional, electrostatic particle-in-cell (PIC) simulations. Recent works have numerically modeled a near-surface environment in one- through three-dimensions (Poppe and Horányi, 2010), including the effect of lunar topographic structures such as a shallow crater (Poppe et al., 2012) and the drop-off of a crater wall (Zimmerman et al., 2011). However, lunar vertical holes have much greater depth-to-diameter ratios than previously examined craters. This large ratio should inhibit solar wind electrons from penetrating into the deep hole, because thermal motion enhances their loss probability at the vertical wall of the hole. This is not the case for SUV radiation and solar wind protons, which exhibit straight and ballistic motions, respectively. Therefore, the surface

 $<sup>* \ \, \</sup>text{Corresponding author}.$ 

charging inside a hole is expected to be different from that outside the hole even for the sunlit face.

The surface charging characteristics inside a hole with a large depth-to-diameter ratio have been an open question. As presented in subsequent sections, our simulations reveal limited solar wind electron penetration into a hole and a complex photoelectron current closure. A very different current balance condition is established inside the hole and the potential at the sunlit hole-bottom surface is higher than outside the hole, which results in a greater potential difference between the sunlit and shadowed regions inside the hole.

#### 2. Numerical model and setup

We have simulated the three-dimensional plasma environment near a vertical hole on the lunar dayside. The simulations were performed using our original plasma particle code called EMSES, originally developed for spacecraft-plasma interaction study (Miyake and Usui, 2009). EMSES is based on the standard electromagnetic PIC method (Birdsall and Langdon, 1985). The plasma is modeled as an aggregation of a huge number of charged macro-particles, whereas the electromagnetic field components are defined discretely on the computational grid points. In the current study, we ran the code in the electrostatic mode, in which Poisson's equation for an electrostatic field and Newton's equations of motion for plasma macro-particles are solved simultaneously as basic equations. EMSES is optimized for efficient computations on modern supercomputers (Miyake and Nakashima, 2013). The code is fully parallelized based on the domain decomposition method, and the computational load imbalance due to plasma non-uniformity is resolved by dynamic load balancing (Nakashima et al., 2009).

The topographical structure of the lunar vertical hole is described as internal boundaries in the simulations. The lunar surface is regarded as an insulator; i.e., the charge of impinging plasma particles is accumulated at their incident positions on the surface. Only the sunlit face of the lunar surface emits photoelectrons at a rate prescribed by an input parameter. As a nominal value, we use a photoelectron current density of  $4.5 \,\mu\text{A/m}^2$  for normal solar incidence (Feuerbacher et al., 1972). The actual photoelectron current from each location on the lunar surface is scaled as  $\cos \psi$ , where  $\psi$  is the angle of solar incidence with respect to the local surface normal. For simplicity, the velocity distribution of photoelectrons is assumed to follow a single Maxwellian distribution with temperature 2.2 eV. We also use the cosine function for modeling the angular distribution of the emission. The emission of each photoelectron creates one positive charge element that remains at the emission position.

In the Cartesian coordinate system used in EMSES, we take the z axis to be the vertical direction and assume an xy (z=0) plane as the lunar plain ground. In the center of the ground, we model a vertical hole with a diameter of 50 m and a depth of 45 m. A plane 60 m under the ground (i.e., 15 m under the bottom surface of the hole) is taken as the lower simulation boundary. The three-dimensional simulation domain consists of 416, 416, and 2080 grid points along the x,y, and z axes, respectively. We solve about  $2.5 \times 10^{10}$  plasma macro-particles throughout the simulations. The grid width of 0.5 m is comparable to the local Debye length near the surface. We employ the Dirichlet boundary condition for the lower and upper simulation boundaries and a periodic condition for the lateral simulation boundaries.

In the series of the simulations, the Sun direction is parameterized in the simulation xz plane. We examined various solar zenith angles  $\theta$  ranging from 1° to 89°. Initially, the simulation domain above the lunar ground is filled with solar wind electrons and protons with a common bulk flow velocity of 450 km/s, density of

5 cm<sup>-3</sup>, and temperature of 8.6 eV. After the simulation starts, the solar wind is continuously injected from the upper simulation boundary, and we run the simulation until a steady-state environment is obtained as a simulation output. In the present investigations, we do not consider effects of the static magnetic field. This simplifying assumption is justified by much larger Larmor radii of solar wind and photoelectrons compared with the spatial scale of the hole.

#### 3. Simulation results

### 3.1. Charging of vertical hole surface

Fig. 1 displays the potential distribution on the lunar surface for solar zenith angle 30°. The potential is referenced to the value at 980 m above the lunar ground, which can be regarded as the space potential in the solar wind. For visibility, we display only the y > 0half of the surface near the hole, because the potential profile is in principle symmetric with respect to the y = 0 plane. The sunlit part of the ground and hole surface is charged positively, ranging from a few to 20 V, while the shadowed region has a negative potential of a few tens of V. At the interface between the sunlit and shaded region, the locally high potential (20 V at maximum) stands out from the rest of the sunlit part. The feature can also be seen as a potential overshoot at the immediate right of the sunlit-shadow boundary, marked with "1" in the subplot of the hole-bottom potential versus x. This overshooting potential greatly amplifies the electric field from the sunlit to shadowed regions. Although not displayed graphically, local maximum fields of 50 and 20 V/m are observed in the simulation at the rim and bottom of the hole, respectively, which are much greater than the field predicted at the edge of a shallow crater (Poppe et al., 2012). As overviewed above, the potential structure near the sunlit-shadow boundary is rather complex. The issue will be revisited later in

The dependence of the lunar surface potential on the solar zenith angle  $\theta$  is examined in the range of 1–89°. Fig. 2 shows the surface potential profiles for selected angles of  $\theta = 5^{\circ}$ , 30°, 60°, and 85°. As expected, the transition of the sunlit-shadow boundary leads to drastic change of a negatively-charged area inside the hole. Since the potential value in each place shows complex dependence on  $\theta$ , it is helpful to see a potential changes at some fixed observation points. In Fig. 3, we show such local potentials depending on the changing  $\theta$ . We selected two positions: one on the lunar ground outside and far from the hole, and the other at (15, 0, -45) m on the hole bottom, the latter of which is indicated by a cross in Fig. 1. At the hole bottom, the interface between the positive and negative surface potentials moves as  $\theta$  changes. This causes a drop-off of the hole-interior potential around 42°. We also identify a local potential ridge at 41°, which results from the passage of the aforementioned potential overshoot at the observation point. The complex behavior between 42° and 45° also reflects the distinctive potential structure near the boundary (see the subplot in Fig. 1), the implications of which will be discussed in a later

A comparison with the hole-exterior potential reveals that the sunlit surface potentials both inside and outside the hole have a decreasing trend with increasing  $\theta$ . For the hole exterior, this trend has been previously identified from photoelectron yield scaling to  $\cos\theta$  (e.g., Poppe et al., 2012). We will show in a later section that changes in the solar wind proton flux into the sunlit surfaces are also important.

The potential of several V observed at the sunlit lunar ground is consistent with previous predictions (Poppe et al., 2012). A remarkable finding is that the sunlit face of the hole bottom has

# Download English Version:

# https://daneshyari.com/en/article/8136081

Download Persian Version:

https://daneshyari.com/article/8136081

Daneshyari.com